ECS Journal of Solid State Science and Technology, **2** (2) R3148-R3152 (2013)
2162-8769/2013/2(2)/R3148/5/$28.00 © The Electrochemical Society

JSS Special Issue on Luminescent Materials for Solid State Lighting

Luminescence Temperature Quenching for Ce^{3+} and Pr^{3+} *d-f* Emission in YAG and LuAG

K. V. Ivanovskikh,[a,b] J. M. Ogiegło,[a] A. Zych,[a,c] C. R. Ronda,[a,d,e] and A. Meijerink[a,z]

[a]*Condensed Matter and Interfaces, Debye Institute for Nanomaterials Science, Utrecht University, 3508 TA Utrecht, The Netherlands*
[b]*Department of Physics and Astronomy, University of Canterbury, Christchurch 8140, New Zealand*
[c]*PM-ABL Solid State Lighting, Emerging Businesses, Advanced Technologies,Performance Materials, Merck KGaA, D-64293 Darmstadt, Germany*
[d]*Philips Corporate Technologies, Research, 5656 AE Eindhoven, The Netherlands*
[e]*Zhejiang University, Centre for Optical and Electromagnetic Research, Hangzhou 310058, China*

The *d-f* emission from Ce^{3+} and Pr^{3+} in garnets is attracting considerable attention, especially in relation to application in white light LEDs and scintillators. An important aspect is the luminescence quenching temperature T_Q. It is not trivial to determine T_Q and to unravel the quenching mechanism. In this paper the T_Q of *d-f* emission for Ce^{3+} and Pr^{3+} are determined by temperature dependent lifetime measurements. The results show a T_Q for Pr^{3+} of 340 K for $Y_3Al_5O_{12}$:Pr^{3+} (YAG:Pr) and 680 K for $Lu_3Al_5O_{12}$:Pr^{3+} (LuAG:Pr). For Ce^{3+} the T_Q is too high to measure. An onset of quenching above 600 K (YAG:Ce) or 700 K (LuAG:Ce) is observed. The differences in T_Q between YAG and LuAG are explained by a smaller Stokes shift for the *d-f* emission in LuAG (~2300 cm^{-1}) compared to YAG (~2750 cm^{-1}) derived from low temperature luminescence spectra. The large difference in T_Q between Ce^{3+} and Pr^{3+} is related to the smaller energy difference between the lowest energetic *fd* state of Pr^{3+} and the next lower $4f^2$ state ($^3P_2$) compared to the $5d - 4f^1(^2F_{7/2})$ energy difference for Ce^{3+}. Both observations are consistent with luminescence temperature quenching by non-radiative relaxation from the 5*d* state to the 4*f* state described by a configurational coordinate diagram and not by thermally induced photoionization.
 [DOI: 10.1149/2.011302jss]

Manuscript submitted September 6, 2012; revised manuscript received October 12, 2012. Published December 6, 2012. *This paper is part of the JSS Special Issue on Luminescent Materials for Solid State Lighting*.

The luminescence quenching of *d-f* emission of lanthanide ions is attracting increasing attention in recent years. Up till about 20 years ago luminescence quenching was explained using the configurational coordinate diagram.[1] Thermally activated cross-over from the excited state to the ground state parabola could explain differences in quenching temperature. Both handwaving arguments (stronger relaxation on a larger cation site causes lower quenching temperatures T_Q) or careful determination of the Stokes shift (larger Stokes shift gives rise to a lower T_Q) were used to justify differences in T_Q.[2] Complex quantitative models were developed based on the overlap of thermally occupied vibrations in the excited state with high vibrational levels of the ground state to accurately describe the temperature dependence of the cross-over rate.[3] However, as more examples were found where observations of differences in quenching temperatures did not agree with expectations based on the configurational coordinate model, another mechanism for temperature quenching was successfully introduced. If the excited 4f5d state is close in energy to the conduction band, the 5d electron may be thermally excited to the conduction band under photoexcitation at elevated temperatures, leading luminescence quenching through thermally activated photoionization.[4] In recent years, the thermally activated photoionization mechanism has become the mechanism of choice to explain luminescence temperature quenching.

An important model system for luminescence of trivalent lanthanide ions is the family of garnet hosts $Ln_3M_5O_{12}$ where Ln can be Y^{3+}, Gd^{3+} or Lu^{3+} (optically not active in the visible spectral range) while the M site can be occupied by Al^{3+} or Ga^{3+}. Luminescent trivalent lanthanides can be incorporated on the Ln^{3+} site. Both for fundamental studies and applications, the variation in cation occupation makes these garnets ideal to tune and model optical properties as a function of covalency, size of the cation site, bandgap, vibrational energies etc. Applications of $Y_3Al_5O_{12}$:Ce^{3+} (YAG:Ce^{3+}) in white light LEDs and $Lu_3Al_5O_{12}$:Ce^{3+} (LuAG:Ce^{3+}) and LuAG:Pr^{3+} as scintillator materials use the flexibility to shift the emission to the red for warmer white LEDs (e.g. by partial replacement of Y by Gd)[5] or for reducing afterglow in scintillator by substitution of Al with Ga.[6] Interesting differences between luminescence quenching temperatures of the *d-f* emission from Ce^{3+} and Pr^{3+} have been observed upon variations on the Ln site and the M site. For the Ce^{3+} T_Q is lowered when Y is replaced by Gd or Tb and this has been explained by the classic configurational coordinate diagram.[7] Replacement of Al by Ga also results in a lower T_Q which was initially explained by the configurational coordinate diagram but recently convincing evidence was presented by careful photoconductivity experiments, showing that upon raising the Ga concentration the bandgap of YAG decreases and for high Ga-concentrations the conduction band is at lower energy than the lowest 5d state ($5d_1$).[8] The results in Ref. 8 clearly demonstrate that thermally activated photoionization causes thermal quenching of the Ce^{3+}-luminescence in systems with elevated Ga-concentrations.

In this paper we investigate the mechanism for thermal quenching of the d-f emission from Ce^{3+} and Pr^{3+} in YAG and LuAG. The quenching temperature T_Q is defined as the temperature at which the radiative decay rate and non-radiative decay rate are equal, which means that the quantum yield has dropped to 50%, assuming a 100% quantum yield at low temperatures. T_Q can be determined by temperature dependent lifetime measurements for low doping concentrations. In a previous study we have shown that this is the most reliable method to determine the quenching temperature and that other methods can easily give erroneous values for T_Q due to thermally activated concentration quenching or changes in the absorption strength with temperature.[9] In addition to determining T_Q high resolution low temperature excitation and emission spectra were recorded to determine the Stokes shift for the *d-f* emission in the different systems. The results show that the luminescence temperature quenching can be explained by the configurational coordinate diagram and that these systems are model systems for demonstrating how subtle changes in the relaxation of the excited state give rise to large differences in quenching temperatures.

Experimental

Sample preparation.— The different samples were synthesized by a modified Pechini method described by Katelnikovas at al.[10]

[z]E-mail: a.meijerink@uu.nl

High purity Y_2O_3, Lu_2O_3, $Al(NO_3)_3 \cdot 9H_2O$, $Pr(NO_3)_3 \cdot 6H_2O$ and $Ce(NO_3)_3 \cdot 6H_2O$ were used as starting materials with citric acid as the complexing agent. In the samples a concentration of 0.1 or 0.3 mole% of Ce^{3+} or Pr^{3+} relative to Y^{3+} or Lu^{3+} was used. The calcinations were performed in two steps at 1000°C for 3 h and 1650°C for 4 h with an intermediate grinding step. To prevent partial oxidation to Ce^{4+} and Pr^{4+}, the second annealing step was carried out under CO. Single phase formation in all samples was confirmed with the X-ray diffraction measurements recorded on Rigaku Miniflex II Equipment.

Optical spectroscopy.— Luminescence spectra were recorded on an Edinburgh Instruments FLS920 fluorescence spectrometer equipped with a 450 W Xe arc lamp and a cooled single photon counting photomultiplier (Hamamatsu R928P). The excitation spectra were corrected for the instrumental response. Low-temperature measurements were carried out using an Oxford Instruments liquid helium flow cryostat. Above room temperature a homemade high temperature cell was used with a limit of about 700 K. The high temperature cell uses a copper block with a heating coil. A thin (~0.3 mm) sample layer is pressed in a small recess in the block and is covered with a thick (3 mm) quartz plate for insulation. The temperature sensor is placed directly under the sample. The difference in the actual temperature of the sample and the temperature sensor will be smaller in the low temperature regime. At high temperatures a small temperature gradient can occur due to (radiative) heat loss from the surface. The quenching temperatures are estimated to have an error below 20 K at temepraturees below 500 K. Above 600 K larger deviations may occur. Luminescence decay curves were recorded using a time correlated single-photon counting (TCSPC) method under excitation with a 270 nm PLS-270 LED ($\lambda_{exc} = 270$ nm, pulse width ~200 ps) for Pr^{3+} d-f emission or diode laser ($\lambda_{exc} = 406$ nm, pulse width ~65 ps) for Ce^{3+} d-f emission with repetition rate of 1 MHz controlled by a PDL-800B driver (PicoQuant). The emitted photons were detected using a high-intensity 0.1 m Bausch&Lomb monochromator equipped with a high-speed H5783P-01 photomultiplier (Hamamatsu). Low-temperature luminescence decay curves were recorded using TCSPC at the Superlumi setup (HASYLAB, DESY) employing a 0.3 m ARC SpectraPro-308i monochromator equipped with a high-speed microchannel plate detector R3809U-50S under excitation with synchrotron radiation. The set-ups used have not been wavelength calibrated over the full spectral region and absolute errors up to 50 cm^{-1} can occur in the reported energies for zero-phonon lines and band maxima.

Results and Discussion

Temperature dependent lifetime measurements.— Luminescence decay curves were recorded in the maximum of the d-f emission bands under direct excitation f-d excitation and were single exponential. The lifetimes values were obtained from single exponential fits and the resulting lifetimes measured at different temperatures are plotted in Figure 1 for YAG:Ce^{3+}, LuAG:Ce^{3+}, YAG:Pr^{3+} and LuAG:Pr^{3+}. The quenching temperature for d-f emission from Ce^{3+} in both YAG and LuAG is very high and is beyond the experimental limit of our set-up. Based on the measurements it is clear that the quenching temperature for Ce^{3+} in LuAG is higher than for Ce^{3+} in YAG. An onset of quenching around 600 K is observed for Ce^{3+} in YAG while for Ce^{3+} in LuAG the onset is shifted to 700 K and it is likely that the T_Q for YAG:Ce^{3+} and LuAG:Ce^{3+} is above 700 and 800 K, respectively. The very high quenching temperatures are in agreement with our previous report on temperature quenching in YAG:Ce^{3+} [9] and with pioneering work, presently often forgotten,[9] by Weber.[11] The temperature dependent lifetimes for the Pr^{3+} emission show a large difference in quenching temperature between YAG and LuAG and a significantly lower T_Q than for the Ce^{3+} emission. The temperature at which the lifetime $\tau_{1/e}$ has dropped to half the initial value is 340 K in YAG, in agreement with Ref. 11, and 680 K in LuAG. The quenching temperature of Pr^{3+} emission in YAG is too low for scintillator application. The onset of the temperature quenching for Pr^{3+} d-f emission is around 150 K in YAG and around 450 K in LuAG. Clearly, the quenching starts at much lower temperatures for d-f emission from Pr^{3+} than from Ce^{3+} in the same host lattice. Summarizing, the temperature dependent life time measurements reveal that the luminescence quenching temperature for d-f emission is higher for Ce^{3+} than for Pr^{3+} and higher for these ions in LuAG than in YAG.

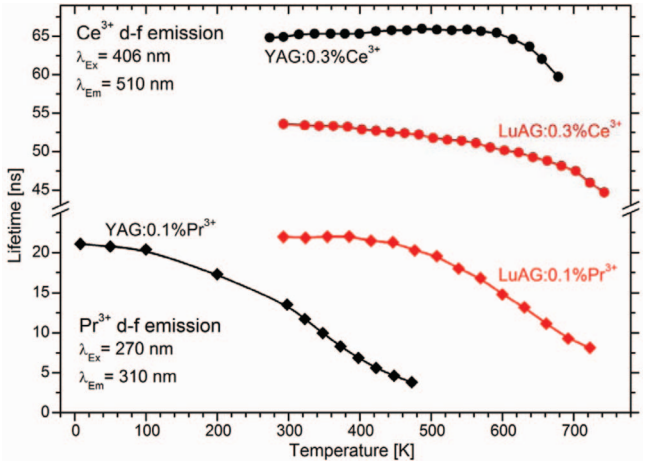

Figure 1. Luminescence lifetimes of Ce^{3+} and Pr^{3+} ions doped into YAG and LuAG as function of temperature. The lifetimes are derived from single exponential decay curves and measured in the maximum of the corresponding d-f emission. Excitation and emission wavelengths are indicated in the Figure.

Low temperature luminescence spectra.— To obtain a better understanding of the quenching mechanism, high resolution spectra were recorded at cryogenic temperatures for samples with low doping concentrations. Under these conditions the true spectral shape of the excitation and emission bands can be observed due to elimination of processes like reabsorption of emission, energy transfer, saturation or inhomogeneous broadening. It is well known that for the *d-f* luminescence spectra for low doping concentrations, zero-phonon lines and vibronic replicas can be observed for Ce^{3+}, Pr^{3+} and Tb^{3+} in YAG and LuAG.[9,12–14] In Figures 2 and 3 the excitation and emission spectra for all four systems are depicted. Information on the maxima of the excitation and emission bands as well as on the bandwidths and Stokes' shifts determined from these data is also gathered in Table I.

The luminescence spectra show a sharp onset and sometimes even a clear zero-phonon line, both in excitation and emission. The emission spectra for Ce^{3+} show the characteristic doublet structure to the splitting of the ^2F ground state by spin-orbit (SO) coupling in a $^2F_{5/2}$ and a $^2F_{7/2}$ state. The typical SO splitting of 2000 cm^{-1} is observed in the emission spectrum due to transitions from the lowest $5d_1$ state to both ^2F_J states. In the excitation spectrum only the transition to the lowest energy 5d state is shown but higher 5d states can be observed in the UV part of the spectrum.[9,12,13] The Stokes' shift measured for the 5d emission of Ce^{3+} in YAG (2812 cm^{-1}) is slightly larger than the Stokes shift reported by us before.[9] From excitation and emission spectra of YAG:0.03%Ce^{3+} recorded at 4 K a Stokes' shift of 2500 cm^{-1} was calculated. The main difference is a slightly higher energy position measured for the maximum of the emission spectrum of YAG:0.03%Ce^{3+}. Possibly, reabsorption of the emission causes a small redshift of the emission in a sample with 0.1% of Ce^{3+}. Note that the zero-phonon lines have a lower relative intensity in emission than in excitation, which can also be explained by reabsorption. The high oscillator strength of f-d transitions causes distortions of the emission spectra, already for low dopant concentrations. For the determination of the Stokes' shift, the value derived from spectra measured for the lower Ce-concentration used in Ref. 9 will be the more accurate value. For the present comparison of Stokes' shifts we will use the values derived for samples which were all doped with 0.1% of Ce^{3+} or Pr^{3+}.

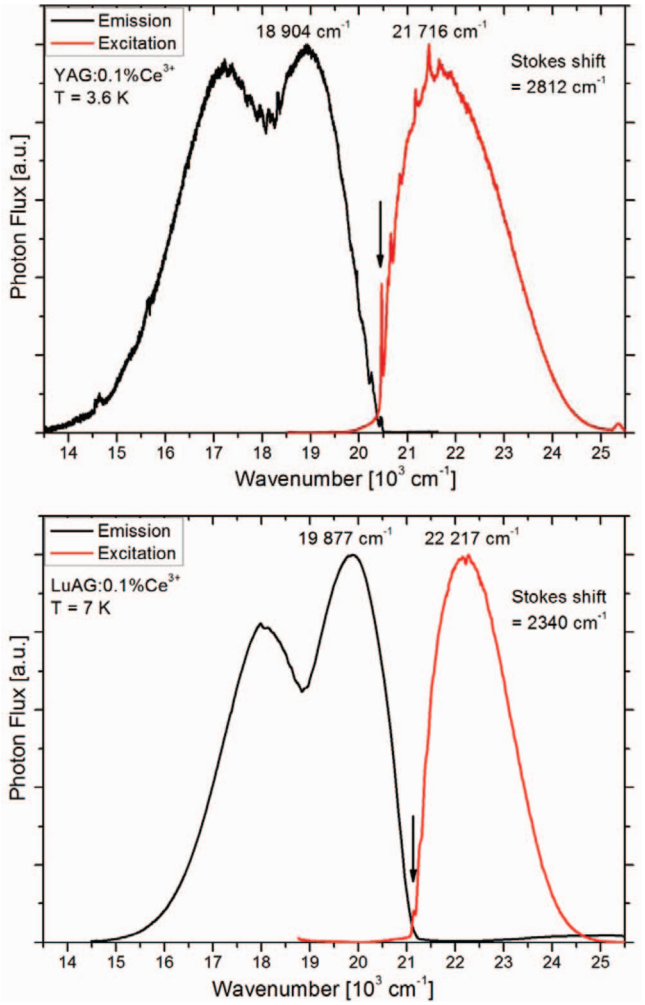

Figure 2. Low temperature excitation and emission spectra for YAG:0.1%Ce^{3+} and LuAG:0.1%Ce^{3+} The spectra reveal clear zero-phonon lines and allow for an accurate determination of the excitation and emission maxima, as well as the Stokes' shift which are included in the figures. Positions of ZPLs are marked by arrows.

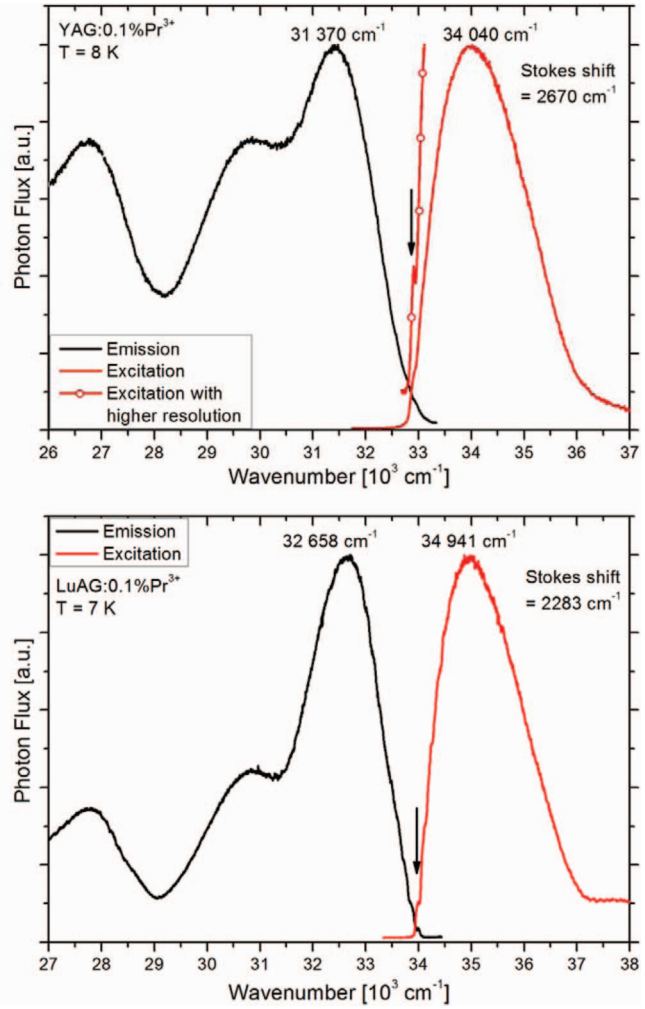

Figure 3. Low temperature excitation and emission spectra for YAG:0.1%Pr^{3+} and LuAG:0.1%Pr^{3+}. The spectra reveal clear zero-phonon lines and allow for an accurate determination of the excitation and emission maxima, as well as the Stokes' shift which are included in the figures. Positions of ZPLs are marked by arrows.

This makes a reliable comparison possible, but the actual Stokes shifts are probably slightly smaller than those tabulated in Table I.

The excitation and emission spectra for Pr^{3+} are shown in Figure 3. In emission two split bands are observed around 32000 cm^{-1} and 27000 cm^{-1}. The emission bands are assigned to transitions from the $5d_1$ level to the $4f^2$ ground state levels $^3H_4$, $^3H_5$ and $^3H_6/^3F_2$, $^3F_3/^3F_4$. In the excitation spectra the transition to the $5d_1$ state (~35000 cm^{-1}) is observed.

The results show a clear difference between the luminescence properties in YAG and LuAG. For both Ce^{3+} and Pr^{3+} the position of the lowest 5d state ($5d_1$) is at ~700 cm^{-1} higher energies, calculated from the positions of the zero-phonon lines (ZPLs). The Stokes' shifts for the d-f emission in YAG (~2750 cm^{-1}) are significantly larger than in LuAG (~2300 cm^{-1}). The smaller relaxation in the fd excited state for Ce^{3+} and Pr^{3+} in LuAG compared to YAG is confirmed by the narrower bandwidth for the 4f-$5d_1$ excitation bands (~1900 cm^{-1} in LuAG vs. ~2300 cm^{-1} in YAG). The observation that the trends in the spectral shifts and Stokes' shifts are similar for Pr^{3+} and Ce^{3+} for the two host lattices is in agreement with the model of Dorenbos which predicts that apart from a general shift of about 12000 cm^{-1} the luminescence properties for the d-f luminescence should be similar in

Table I. Characteristics of the luminescence measured for Ce^{3+} and Pr^{3+} in YAG and LuAG for low (0.1%) doping concentrations and low temperatures. The maxima for the 4f-$5d_1$ excitation and emission band, the Stokes' shift (SS) and full width at half maximum (FWHM) for the 4f-$5d_1$ excitation band are tabulated. In addition, the quenching onset and luminescence quenching temperatures (T_Q) derived from temperature dependent lifetime measurements are included.

Activator	Host	$5d_1$ exc (cm^{-1})	$5d_1$ em (cm^{-1})	SS (cm^{-1})	FWHM (cm^{-1})	ZPL (cm^{-1})	Quenching onset (K)	T_Q (K)
Ce^{3+}	YAG	21716	18904	2812	2400	20424	~600	>700
	LuAG	22217	19877	2340	1900	21137	~700	>800
Pr^{3+}	YAG	34040	31370	2670	2200	32910	~150	~340
	LuAG	34941	32658	2283	1950	33996	~450	~680

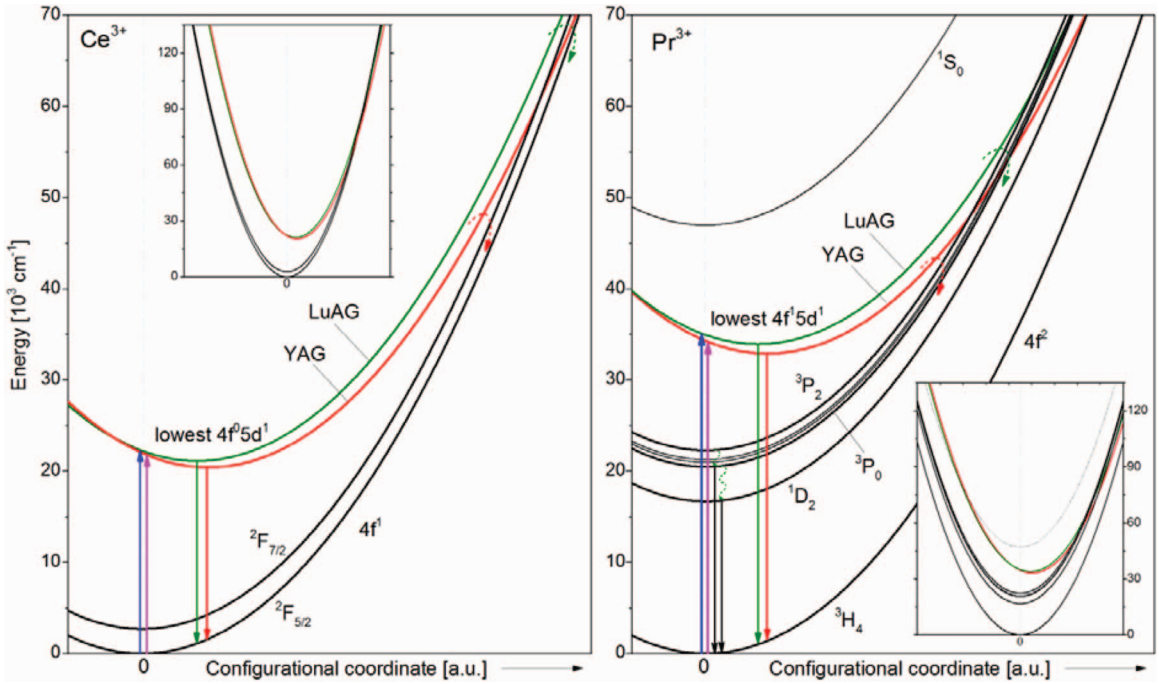

Figure 4. Configurational coordinate diagrams explaining quenching mechanisms for Ce^{3+} and Pr^{3+} 5d-4f emission in YAG and LuAG. The diagrams are drawn to scale to match the actual energies measured for the zero-phonon lines and the emission and excitation maxima.

the same host lattice.[15,16] Based on the Stokes shift and bandwidth it is clear that the relaxation in the 5d excited state is smaller for the 5d excited state of Ce^{3+} and Pr^{3+} in LuAG.

Luminescence quenching mechanism.— The differences observed in luminescence spectra provide insight in the mechanism responsible for luminescence temperature quenching of d-f emission from Pr^{3+} and Ce^{3+} in YAG and LuAG. First, we consider quenching through thermally activated photoionization. For this mechanism the energy difference between the emitting $5d_1$ state and the bottom of the conduction band (CB) determines the quenching temperature. The position of the $5d_1$ level with respect to the CB is expected to be similar for Pr^{3+} and Ce^{3+}. Experimental evidence has been provided by Dorenbos.[15,16] The constant energy difference can be understood from the limited influence of extra electrons within the $4f^n$ core (the only difference between lanthanide ions) on the energy of the 5d electron. In this model a similar quenching temperature is expected for d-f emission from Ce^{3+} and Pr^{3+} since quenching is caused by thermally activated escape of an electron from the $5d_1$ level to the conduction band. The fact that T_Q is varies strongly, indicates that it is highly unlikely that photoionization is the operative quenching mechanism. For Ce^{3+} the energy difference between $5d_1$ state and the bottom of the conduction band has been estimated to be 10000 cm^{-1}.[17] This large energy barrier for photoionization provides further confirmation that this is not the quenching mechanism.

In the configurational coordinate model the quenching temperature depends on the Stokes' shift (a larger offset between the ground state and excited state parabola gives a larger Stokes' shift and a lower T_Q) and the energy difference between emitting state and the next lower state to which relaxation can occur. A smaller energy difference results in a lower T_Q. The observations in Figs. 1–3 are consistent with quenching through thermally induced relaxation from the excited $5d_1$ state parabola to the next lower 4f parabola. The energy difference between the emitting $5d_1$ state and the next lower 4f state is much larger for Ce^{3+}. For Ce^{3+} the $5d^1$ state is at 20800 cm^{-1} (average from the ZPLs in YAG and LuAG) and the highest $4f^1$ level ($^2F_{7/2}$) is around 2000 cm^{-1}; so the energy difference is about 18800 cm^{-1}. For Pr^{3+} the $5d_1$ state is at much higher energies (33500 cm^{-1} average energy of ZPLs) but the highest $4f^2$ state to which relaxation can occur is the $^3P_2$ state around 22500 cm^{-1} which gives an energy gap of only 11000 cm^{-1}. Evidence for quenching by cross-over from the $5d_1$ state to the $^3P_2$ states for Pr-doped LuAG and YAG has been discussed in Ref. 18. The large difference in energy gap between Ce^{3+} and Pr^{3+} (18800 vs. 11000 cm^{-1}) explains the higher T_Q for the d-f emission from Ce^{3+} in comparison to Pr^{3+} in the same host lattice. This is especially clear in YAG where T_Q is 340 K for Pr^{3+} and there is no temperature quenching for Ce^{3+} until an onset at 600 K.

The second parameter which strongly influences T_Q in the configurational coordinate diagram model is the relaxation in the excited state. A larger Stokes' shift, indicating stronger relaxation, results in a lower quenching temperature in the configurational coordinate model. In cases where no relation between T_Q and the Stokes' shift is observed, this is often held as evidence for photoionization. Comparison of the luminescence spectra reveals a significantly larger Stokes' shift for the d-f emission of both Ce^{3+} and Pr^{3+} in YAG compared to LuAG. The larger relaxation in the excited fd state for Ce^{3+} and Pr^{3+} in YAG is confirmed by a larger bandwidth of the $5d_1$ excitation bands in YAG. In agreement with the configurational coordinate model, the quenching temperatures are much lower for the d-f emission in YAG. For Pr^{3+} in YAG T_Q is 340 K while for Pr^{3+} in LuAG, where the Stokes' shift is ~400 cm^{-1} smaller, T_Q has increased to 680 K. Note that also the shift of the $5d_1$ state to higher energies contributes to a higher T_Q due to an increased energy gap to the $^3P_2$ state. Also for Ce^{3+} a higher T_Q is observed in LuAG than in YAG although, since the quenching occurs at the temperature limit of the experimental set-up, the difference is not as clear.

The analysis of the luminescence spectra and temperature quenching shows that the configurational coordinate model can explain the quenching of the d-f luminescence from Ce^{3+} and Pr^{3+} in YAG and LuAG. In Figure 4 the configurational coordinate diagram is drawn for Ce^{3+} and Pr^{3+} in YAG and LuAG. The diagrams are drawn to fit the experimental data with the same curvature for the parabolas (same bond strength) in the 4f ground state and 5d excited state. The energy difference between the minima of the parabolas is equal to the zero-phonon line energy and the maxima in excitation and emission spectra are used to determine the transition energies from

the middle of the zero-vibrational level (equilibrium distance) to the parabola above (excitation) or below (emission). The diagrams are very similar and demonstrate that a subtle difference in excited state relaxation can give rise to large differences in luminescence quenching temperature. The systems may serve as model systems for modeling temperature quenching and ab initio calculations which can calculate the potential energy landscape of excited fd states for lanthanide ions.[19]

Conclusions

The luminescence quenching temperature has been determined for d-f emission of Ce^{3+} and Pr^{3+} in YAG and LuAG. A large variation in quenching temperatures T_Q (340 K for YAG:Pr^{3+}, 680 K for LuAG:Pr^{3+}, >700 K for YAG:Ce^{3+} and >800 K for LuAG:Ce^{3+}) is observed. The differences in T_Q can be related to parameters derived from high resolution luminescence spectra based on quenching described by a configurational coordinate diagram model. The garnets can serve as model systems for providing a better theoretical understanding of luminescence quenching mechanisms.

References

1. B. Henderson and G. F. Imbusch, *Optical Spectroscopy of Inorganic Solids*, Oxford Science Publication, Clarendon Press, Oxford (1989).
2. G. Blasse and B. C. Grabmaier, *Luminescent Materials*, Springer Verlag, Berlin (1994).
3. C. W. Struck and W. H. Fonger, *Understanding luminescence spectra and efficiency using W_p and related functions*, Springer, Berlin (1991).
4. M. Raukas, S. A. Basun, W. Van Schaik, W. M. Yen, and U. Happek, *Appl. Phys. Lett.*, **69**, 3300 (1996).
5. S. S. Zhang, W. D. Zhuang, C. L. Zhao, Y. S. Hu, H. Q. He, and X. W. Huang, *J. Rare Earths*, **22**, 118 (2004).
6. M. Nikl, J. Pejchal, E. Mihokova, J. A. Mares, H. Ogino, A. Yoshikawa, T. Fukuda, A. Vedda, and C. D'Ambrosio, *Appl. Phys. Lett.*, **88**, 141916 (2006).
7. C. C. Chiang, M. S. Tsai, and M. H. Hon, *J. Electrochem. Soc.*, **155**, B517 (2008).
8. J. Ueda, S. Tanabe, and T. Nakanishi, *J. Appl. Phys.*, **110**, 053102 (2011).
9. V. Bachmann, C. R. Ronda, and A. Meijerink, *Chem. Mater.*, **21**, 2077 (2009).
10. A. Katelnikovas, J. Barkaukas, F. Ivanauskas, A. Beganskiene, and A. Kareiva, *J. Sol-Gel Sci. & Tech.*, **41**, 193 (2007).
11. M. Weber, *Solid State Comm.*, **12**, 741 (1973).
12. D. J. Robbins, B. Cockayne, J. L. Glasper, and B. Lent, *J. Electrochem. Soc.*, **126**, 1213 (1979).
13. D. J. Robbins, *J. Electrochem. Soc.*, **126**, 1550 (1979)
14. A. K. Zych, J. Ogieglo, C. R. Ronda, C. de Mello Donega, A. Meijerink, and J. Lumin, Accepted for publication.
15. P. Dorenbos, *J. Lumin.*, **108**, 301 (2004).
16. E. van der Kolk, P. Dorenbos, C. W. E. van Eijk, S. A. Basun, G. F. Imbusch, and W. M. Yen, *Phys. Rev. B*, **71**, 165120 (2005).
17. D. S. Hamilton, S. K. Gayen, G. J. Pogatshnik, R. D. Ghen, and W. J. Miniscalco, *Phys. Rev. B*, **39**, 8807 (1989).
18. J. Pejchal, M. Nikl, E. Mihokova, J. A. Mares, and A. Yoshikawa et al., *J. Phys. D: Appl. Phys.*, **42**, 055117 (2009).
19. A. B. Munoz-Garcia, J. L. Pascual, Z. Barandiarán, and L. Seijo, *Phys. Rev. B*, **82**, 064114 (2010).